Effect of turbine alignment on the average power output of wind-farms

Richard J. A. M. Stevens[1,2], **Dennice F. Gayme**[1] **and Charles Meneveau**[1]
[1]Dept. of Mech. Engineering, Johns Hopkins University, Baltimore, Maryland 21218, USA
[2]Dept. of Physics, Mesa+ Institute, and J. M. Burgers Centre for Fluid Dynamics, University of Twente, 7500 AE Enschede, The Netherlands

Abstract

Using Large Eddy Simulation (LES), we investigate the influence of the alignment of successive turbine rows on the average power output of a finite length wind-farm with a stream-wise spacing between the turbines of $S_x = 7.85D$ and a span-wise spacing of $S_y = 5.23D$, where D is the turbine diameter. Different turbine alignments affect the extent to which wakes from upstream turbines interact with downstream turbines. We consider 13 turbine rows in the stream-wise direction and change the layout of the wind-farm by adjusting the angle $\psi = \arctan \frac{S_{dy}}{S_x}$ with respect to the incoming flow direction, where S_{dy} indicates the span-wise offset from one turbine row to the next. For the case considered here, $\psi = 0$ degrees corresponds to an aligned wind-farm, while a perfectly staggered configuration occurs at $\psi = \arctan[(5.23D/2)/7.85D] = 18.43$ degrees. We simulate the interaction between each wind-farm and the atmospheric boundary layer using a LES that uses a newly developed concurrent-precursor inflow method. For an aligned configuration we observe a nearly constant average turbine power output for the second and subsequent turbine rows, which is about 60% of the average power produced by the turbines in the first row. With increasing ψ the power loss in subsequent turbine rows is more gradual. We find that the highest average power output is not obtained for a staggered wind-farm ($\psi = 18.43$ degrees), but for an intermediate alignment of around $\psi = 12$ degrees. Such an intermediate alignment allows more turbines to be outside the wake of upstream turbines than in the staggered configuration in which turbines are directly in the wake of turbines placed two rows upstream.

Introduction

At the end of 2011 almost 3% of global electricity demand came from wind power (1) and various scenarios (2; 3) aim for this contribution to increase to 20% by 2030. Several countries have already achieved a relatively high usage of wind power in 2011, such as 26% in Denmark, and 16% in Portugal and Spain (4). To realize the worldwide targets for wind power production large wind-farms will be required.

The problem can be approached at many different spatial and temporal scales. From the perspective of atmospheric dynamics on large regional or global scales wind turbine arrays are often modeled as surface roughness elements or net drag coefficient. This parameterization leads to an increased roughness length that needs to be parameterized. This approach is useful,

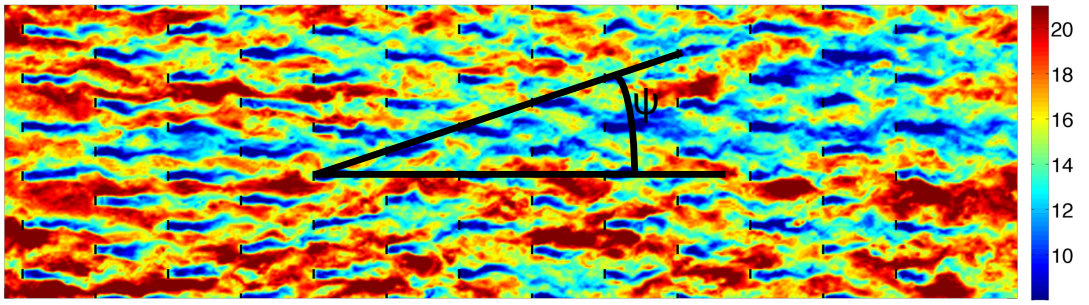

Figure 1: Snapshot of the stream-wise velocity at hub-height in a staggered wind-farm in which the stream-wise distance between the turbines is $S_x = 7.85D$ and the span-wise distance is $S_y = 5.23D$. The wind-farm layout is parameterized by the angle $\psi = \arctan \frac{S_{dy}}{S_x}$ with respect to the incoming flow direction, where S_{dy} indicates the span-wise displacement and S_x is the stream-wise distance between the subsequent rows, indicates the wind-farm layout. The color scale indicates u/u^*, the stream-wise wind velocity in units of friction velocity.

among others, in simulations in which the effect of large wind-farms at regional and global scales is considered. Examples are studies that aim to predict the effect of large wind turbine farms on the global climate (5; 6), regional meteorology (7), or short time weather patterns (8; 9). In such simulations, the horizontal computational resolution near the ground is often significantly coarser than the height of the Atmospheric Boundary Layer (ABL) and therefore insufficient to study the physical mechanisms that are important in large wind-farms. RANS (Reynolds-averaged Navier-Stokes) simulations have traditionally been the main tool to model large wind-parks (10; 11), but recently Large Eddy Simulations (LES) of the interaction between wind turbines and the turbulent ABL have become available (10).

There are several LES studies that model the interaction between one or two turbines and the ABL (12; 13; 14; 15; 16; 17; 18; 19; 20). However, only a limited number of LES have focused on large wind turbine parks. Ivanell (21) performed LES of two of the ten rows of the Horns Rev farm in Denmark and assumed periodic conditions in the span-wise direction to approximate the full plant aerodynamics. That work employed a power law profile for the mean wind inflow condition and a plane of fluctuating body forces parallel to and near the upstream boundary to create turbulence. In that study the wind inflow angle was varied by $\pm 15^\circ$ with respect to the alignment of the turbine rows. Churchfield et al. (22; 23; 24) used LES to model the Lillgrund wind-farm plant using a precursor simulation of an ABL to generate the turbulent inflow condition. The time-averaged power production of the turbines for their simulation of a wind-farm with aligned rows agrees well with field observations up to the sixth turbine row. Meyers and Meneveau (25) and Calaf et al. (26; 27) performed LES in a horizontally periodic domain in order to study infinitely long wind-farms. They looked at the effect of the spacing between the wind turbines on the total average power output and the scalar transport. Their results showed that in infinite wind-farms the total average power output is mainly determined by the vertical fluxes of kinetic energy in the wind-farm, which was confirmed in the wind tunnel experiments of Cal et al. (28). Later Yang et al. (29) showed that in infinite aligned wind-farms the stream-wise spacing has a stronger influence on the average power output than the span-wise

spacing. Wu and Porté-Agel's (30; 31) simulations of finite length wind-farms demonstrated that when successive turbine rows are staggered (i.e. turbines are aligned with those two rows ahead of them) the relatively longer separation between consecutive downwind turbines allows the wakes to recover more, thus exposing the turbines to higher local wind speeds and lower turbulence intensity levels compared to an aligned farm. Just as Churchfield et al. (22; 23; 24) they used a separate precursor simulation to obtain the turbulent inflow conditions.

Method

Here we discuss the influence of turbine alignment on the average power output of wind turbines in a finite length wind-farm in which the stream-wise distance between the turbines is $S_x = 7.85D$ and the span-wise spacing is $S_y = 5.23D$, where D is the turbine diameter. The diameter and hub-height of the considered turbines is 100m. The domain size we use is 12.57 km x 3.14 km x 2 km in the stream-wise, span-wise and vertical direction and we use a roughness height of $5 \times 10^{-5} L_z$ (where $L_z = 2km$ is the domain height) and a computational grid with $1024 \times 128 \times 256$ computational points. We consider a wind-farm with 13 turbine rows in the stream-wise direction and 6 turbines in the span-wise direction. We change the wind-farm layout by adjusting the angle $\psi = \arctan \frac{S_{dy}}{S_x}$ with respect to the incoming flow direction, where S_{dy} indicates the span-wise displacement of subsequent downstream turbine rows, as illustrated in figure 1. For the configuration specified above $\psi = 0$ degrees corresponds to an aligned wind-farm, while $\psi = \arctan[(5.23D/2)/7.85D] = 18.43$ degrees corresponds to a staggered on. In all of the studies considered herein, the area covered by our wind-farm remains constant, and we look at the influence of the layout of the wind-farm on the average power production.

We simulate the different finite length wind-farms with a recently developed concurrent-precursor method (32). This method considers two interacting computational domains simultaneously, i.e. in one domain a turbulent ABL is simulated in order to generate the turbulent inflow conditions for a second domain in which wind turbines are placed. In each domain we consider a neutral ABL and solve the filtered incompressible Navier-Stokes (NS) equations together with the continuity equation. This means that stratification effects and changes in the wind direction over time are not included. The dynamic Lagrangian scale-dependent Smagorinsky model is used to calculate the subgrid-scale stresses (33). In our code the skew-symmetric form of the NS equation is implemented, which uses a spectral discretization in the horizontal directions and a second-order finite differencing scheme in the vertical direction. A second-order accurate Adams-Bashforth scheme is used for the time integration. The top boundary uses zero vertical velocity and a zero shear stress boundary condition. At the bottom surface a classic imposed wall stress boundary condition relates the wall stress to the velocity at the first grid point and in the span-wise direction we use periodic boundary conditions. The turbines are modeled using an area average actuator disk method (12; 26; 27; 32).

In the remainder of this paper we first compare the current LES results with field measurements from Horns Rev and other model results, and then discuss the influence of the alignment of the turbine rows on the average power production of the wind-farm.

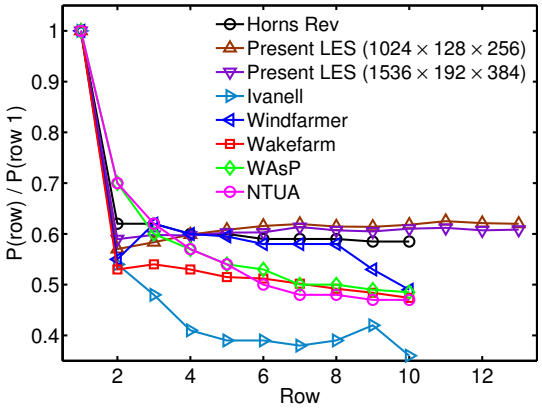

Figure 2: Comparison of the average power output as function of the downstream position between field measurements in Horns Rev, our LES, LES results from Ivanell (21), and several models. Adapted from figure 5 of Ref. (10). Note that the Wakefarm model results have been updated based on Fig. 11.13 of Ref. (37).

Comparison with other data

To evaluate the quality of the LES used in the present work we compare the average power output as function of the stream-wise position downstream of the first turbine position with field measurements fro Horns Rev. The span-wise and stream-wise distance between the turbines used in this study are comparable to the ones used in Horns Rev (34), but not exactly the same. These differences could have some influence on the absolute values, but presumably not on the observed trends. Figure 2 shows that our LES results compare very well with the Horns Rev field measurements. In particular, one can see that our LES correctly captures the nearly constant average power output as function of the downstream position for the second and subsequent rows. Note that such a behavior was also observed in wind tunnel studies by Wu and Porté Agel (31) as well as in their LES results. The average power output in the fully developed regime (as will be seen later, for most cases we approach a fully developed regime in our LES near the 10^{th} row) is likely to have some dependence on the model parameters. It should be noted that there is some uncertainty in the field measurements taken in Horns Rev. (35; 34; 10), which show variations in the average power output in the fully developed regime on the order of 6%, with a standard deviation of about 15%. Nevertheless, the trend observed in the mean power output data, i.e. the almost constant average power for the second and subsequent downstream, is similar in all reported measurements for aligned wind conditions and is well predicted by our LES.

This nearly constant average power as function of the down stream position is due to the complex interaction between the turbines and the ABL. The average power output of downstream turbines is mainly determined by the wake recovery, which depends on the vertical kinetic energy flux that is created by the turbine wakes. In order to capture this large scale phenomenon one needs to accurately model the properties of the ABL and our LES seem to capture these

processes well. Figure 2 shows some differences between the LES of Ivanell (21), who only simulated the two central columns, and the Horns Rev measurements. In Ref. (21), this effect is attributed to the sensitivity of the downstream average power production to the alignment of the wind with respect to the turbines and it is pointed out that there is a significant uncertainty in this alignment in the measurement data. However, they also use a different subgrid scale model and method to generate the turbulent inflow condition than we do in our simulations and this could also account for some of the observed differences.

A number of engineering models have also been proposed to capture the wake effects in large scale wind-farms. A comparison of different studies along with the Horns Rev data is presented in figure 5 of Sanderse et al. (10) and figure 6 of Ref. (36) and this information is also presented in figure 2 together with updated results from Ref. (37). A description of the main features of the models is given by Barthelmie et al. (34). The models vary in the level of detail (complexity) but in general they use some empirical relation for the interacting wakes and/or solve some form of the RANS equations with a $k-\varepsilon$ turbulence closure scheme. It is worth noting that considering the inherent uncertainties in experimental data the agreement between these engineering models and the field measurements is reasonably good. Averaging over wider wind angles significantly improves the results obtained by the models, for example the the Farmflow model shows excellent agreement with Horns Rev data when the wind directions are averaged over 255 to 285 degrees (37). Barthelmie et al. (34), who presented the comparison of these models with the Horns Rev data, mention that although standard models perform adequately for the prediction of wakes in small wind-farms the models seem to have difficulties in predicting the behavior in large multi-row wind-farms when standard parameters are used. They indicate that the interaction of turbulence generated by wind turbines wakes with the overlying atmosphere could be the reason for this. These interactions can be modeled better with LES than by RANS models as LES are better able to predict the unsteady, anisotropic turbulent atmosphere. In addition, the concurrent precursor method we use to generate the turbulent inflow condition is able to capture the time-evolving streaky structures that are natural in an ABL, but difficult to include in synthetic models or in statically swept spatial fields, which is important to accurately model the interaction between the ABL and a wind-farm (32). Therefore we consider LES to be a good research tool to obtain insights about the physical processes that are important in very large wind-farms. We remark on two important assumptions of the present study: it considers only neutral atmospheric conditions (no stratification), and the overall inflow velocity direction is held constant in time. Under realistic conditions, additional meandering of the overall inflow direction would be expected to generate some smearing over results covering a range of angles ψ. In the remainder of this paper we will use LES to consider the effects of wind turbine layout on the average power production in a finite length wind-farm.

Results

We study the effect of the turbine alignment with respect to the incoming flow on the average power output by adjusting the angle ψ, shown in figure 1. Note that changing the wind-farm layout in this way makes sure that the land area that is covered as well as the total number of turbines remains constant. The average power output is evaluated according to $P = \langle -FU_d \rangle$, where $F = -\frac{1}{2}C_T'\rho U_d^2 A$ is the local force used in the actuator disk model. Here U_d is the disk

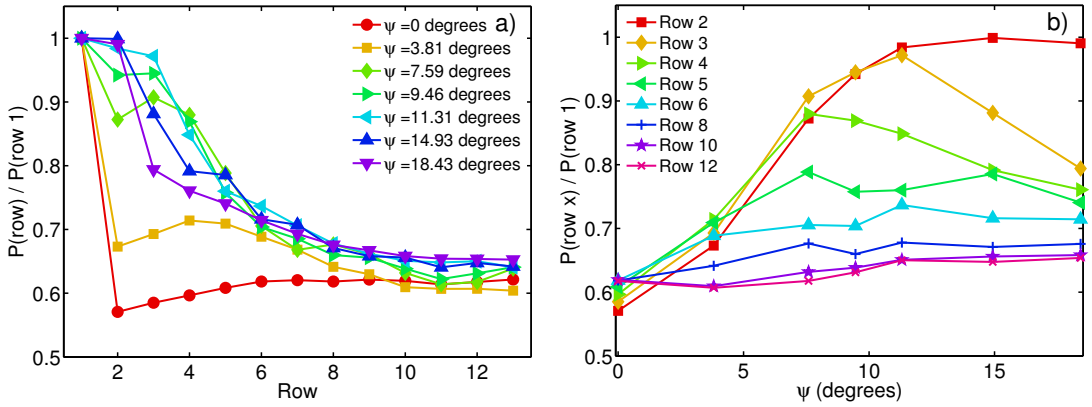

Figure 3: Panel a shows the average power output per turbine normalized by the average power output of turbines in the first row as function of the downstream position for different alignment angles ψ. Panel b shows the average power output in the different rows as function of the alignment angle ψ. Here $\psi = 0$ indicates that the turbines in the wind-farm are aligned and $\psi = 18.43$ corresponds to the fully staggered configuration

averaged velocity, $A = \pi D^2/4$ is the turbine rotor area, ρ is the density of the fluid, and $C_T^{'} = C_T/(1-a)^2$, where a is the axial induction factor. Using typical values $C_T = 4/3$ and $a = 1/4$ leads to $C_T^{'} = 4/3$ (26; 27; 38; 12; 39). Figure 3a shows the averaged normalized power output as function of the downstream position for the different alignments. This figure reveals that for an aligned wind-farm there is a very strong drop in the average power production at the second turbine row and then the average power output from each row remains nearly constant for subsequent downstream turbines. With increasing ψ the power loss in the first couple of rows is more gradual until we get to $\psi = 11.31$ degrees and then the slope begins to increase again. Thus, the staggered arrangement does not necessarily generate the highest average wind-farm power output.

In order to understand this effect it is helpful to look at the data in a different way. Figure 3b shows the normalized power output as function of the alignment angle ψ for the different turbine rows. For the second turbine row the figure reveals a significant power loss for the aligned or nearly aligned cases, while the average power output approaches the value of the first turbine row for the staggered configuration (18.43 degrees). It is important to note that an alignment angle of 11.31 degrees is already sufficient to make sure that the power production at the second row is not hindered by the wakes created by the turbines in the first row. Thus for a wind-farm with two turbine rows the power output will be the same for any alignment angles between 11.31 and $\psi = 18.43$ degrees. However, the alignment becomes much more important for longer wind-farms. The power output of the third turbine row as function of the alignment angle ψ reveals an optimum around $\psi \approx 11.31$ degrees. Interestingly the power output of the third turbine row is approximately equal to the power output of the second row when $0 < \psi \lesssim 11.31$ degrees, while the power output is significantly lower in the third row than at the second row when $\psi \gtrsim 11.31$ degrees.

In order to understand these observation we show the time-averaged stream-wise velocity

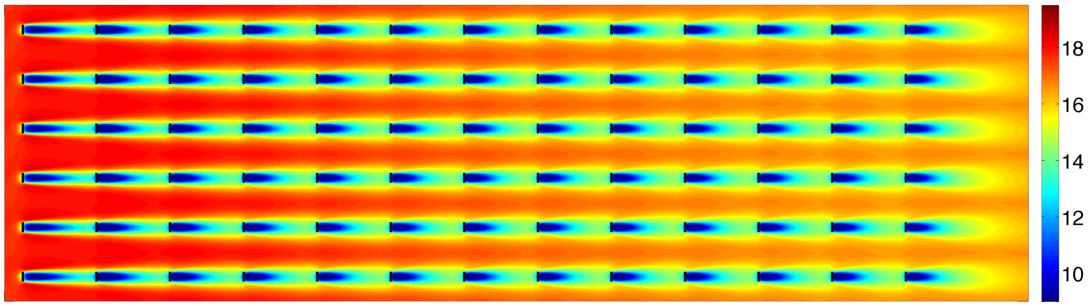

(a) 0 degrees (aligned)

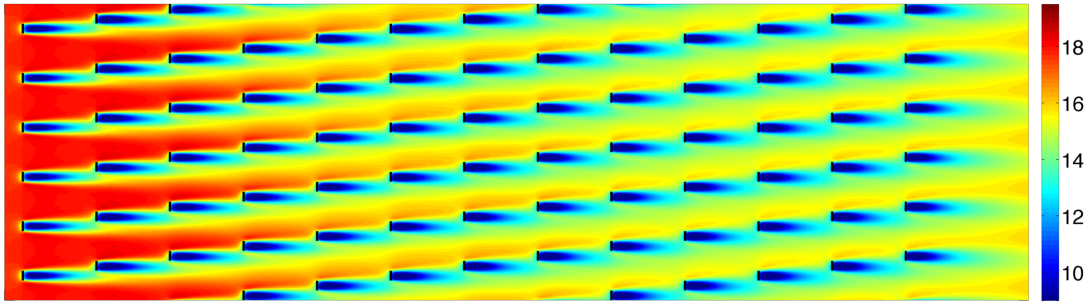

(b) 7.59 degrees (highest power output in fourth row)

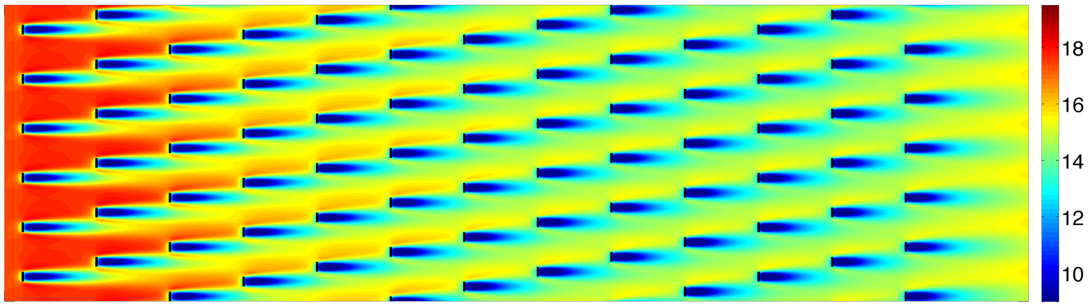

(c) 11.31 degrees (highest power output in third row)

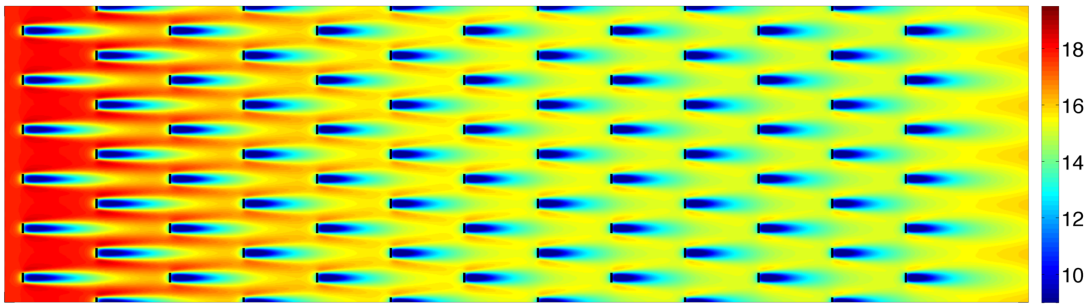

(d) 18.43 degrees (staggered)

Figure 4: The time-averaged stream-wise velocity at hub height for (a) $\psi = 0$ degrees (aligned) (b) $\psi = 7.59$ degrees (highest average power output in fourth row) (c) $\psi = 11.31$ degrees (highest average power output in the third row and for the entire wind-farm) and (d) $\psi = 18.43$ degrees (staggered). The color scale indicates u/u^*, the averaged stream-wise wind velocity in units of friction velocity.

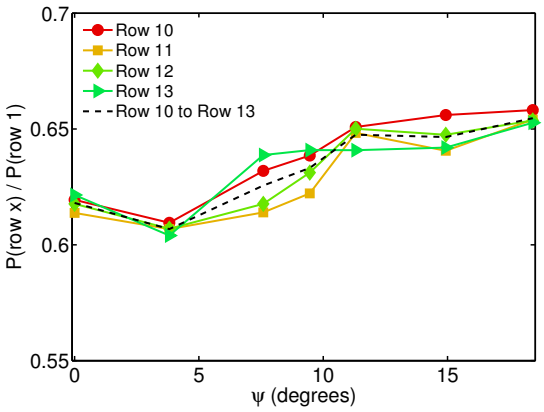

Figure 5: The normalized averaged turbine power output as function of the alignment angle ψ in the fully developed regime of the wind-farm.

at hub height for several cases in figure 4. As periodic boundary conditions in the span-wise direction are used all statistics are periodic in this direction. To improve the statistics we have therefore averaged the stream-wise velocity in $1/6^{th}$ of the original span-wise domain, i.e. the periodicity imposed by the turbines, and subsequently this averaged velocity profile is shown over the original span-wise domain (40). The figure reveals that for $\psi \lesssim 11.31$ degrees the turbines in the first three rows influenced only by the wakes created by turbines directly upstream. For the $\psi = 11.31$ degrees case, which gives the highest power output for turbines on the third row, one can see that both the turbines in the second and third row experience a nearly undisturbed inflow as the alignment angle ψ is sufficient to ensure that the wake of the upstream turbines do not influence them. For smaller alignment angles the turbines experience some negative effect of the expanding and meandering wakes of the upstream turbines. For $\psi \gtrsim 11.31$ the turbines in the third row are starting to encounter the wake created by the first turbine row and for the staggered configuration (18.43 degrees) the turbines in the third row are directly in the wake of those in the first turbine row, which limits the power production of these turbines.

Figure 3b reveals that the power output in the fourth turbine row is highest for an alignment angle of $\psi = 7.59$ degrees. Figure 4 shows that for $\psi = 11.31$ degrees the average power production in the fourth turbine row is limited due to the effect of the wake created by the first turbine row. With the more moderate $\psi = 7.59$ degrees the turbines in the fourth turbine row are not influenced by the wakes created by the turbines in the first row and only feel the meandering wake created by turbines in the third row. For further downstream turbine rows a small further reduction of the turbine power output is observed when $\psi > 0$ degrees. The reason is that the average kinetic energy that is available at hub height slowly decreases inside the wind-farm. Therefore the average wind speed that reaches the subsequent downstream turbines gradually decreases, as is seen in figure 4b and figure 4c, until the fully developed regime is reached. In this fully developed regime the vertical kinetic energy flux that is created by the turbine wakes supplies the power that is extracted by the turbines (26; 28) and the turbine power output seems nearly independent of the angle ψ, as seen in figure 3b. However, figure 5 shows that there are some small differences in this fully developed regime. This figure shows that the average power

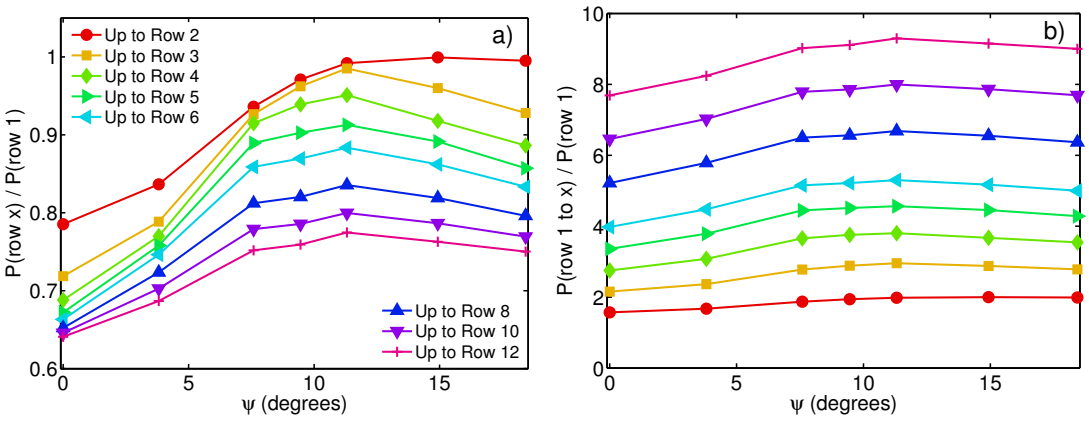

Figure 6: Panel a shows the average power output per turbine normalized by the average power output of turbines in the first row for different wind-farm lengths as function of the alignment angle ψ and panel b shows the total power output for different wind-farm lengths normalized by the power output of the first turbine row.

output is highest for the staggered case. As pointed out by Wu and Porté-Agel (31), this effect can be explained by the longer recovery length that is available for the wakes in the staggered case as compared to the aligned case.

So far we have seen that the highest power output that is found at a particular turbine row depends on the alignment. In particular, in the third row the highest power output is obtained with an alignment angle of $\psi = 11.31$ degrees, whereas the maximum occurs at $\psi = 7.59$ degrees in the fourth row, and in the fully developed regime for a staggered configuration ($\psi = 18.43$ degrees). Therefore one may wonder which wind-farm layout gives the highest power output for the whole wind-farm. Assuming that the power output of turbines is not influenced by downstream turbines we can calculate the average power output per turbine for different wind-farms lengths. Figure 6 shows the average power output per turbine normalized by the power produced by turbines on the first row for wind-farms ranging from 2 to 13 turbine rows as function of the alignment angle ψ. The highest average power output is obtained for the $\psi = 11.31$ degrees case. Figure 6a shows that for a wind-farm with 13 rows in the stream-wise direction the average turbine power output can range from approximately 60% up to about 75% of the power output of the first row. Figure 6b shows the corresponding total power output for different wind-farm lengths normalized by the power output of the first row.

Figure 7 shows the average power output per turbine for different wind-farm length normalized by the power output of an aligned wind-farm of the same length. It shows that the effect of the alignment is strongest for wind-farms with four turbine rows, where an increase in the power production of about 40% is observed for the $\psi = 11.31$ case with respect to the aligned case. For shorter wind-farms the relative increase is lower as a smaller percentage of wind turbines are affected by wake effects. For longer wind-farms the relative power output increase that can be obtained with respect to the aligned cases decreases as the power output in rows further downstream depends less on the orientation than in the first rows.

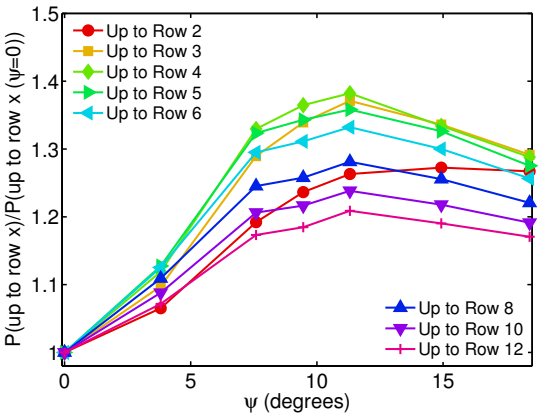

Figure 7: The averaged turbine power outputs for different wind-farm length normalized by the power output obtained by an aligned wind-farm of that length.

Conclusion

Here we discussed the use of Large Eddy Simulations (LES) to study finite length wind-farms. We have seen that the LES is capable of capturing the main trends observed in field experiments. The availability and flexibility of the simulations can therefore be exploited to study large wind-farms in more detail. We studied the effect of the wind-farm layout, parametrized by the alignment angle ψ with respect to the incoming flow, on the average power output of a wind-farm. With fixed land area our results show that under very specific circumstances and depending on the wind-farm length, the average power output of the wind-farm can reach values 40% higher than the power output of an aligned wind-farm. Interestingly the highest average power output is not necessarily obtained for a staggered wind-farm (18.43 degrees in this case), but for an intermediate angle of 11.31 degrees. It is important to stress that each of these results have been obtained using a single inflow direction. In realistic applications, one should average over different inflow directions, depending on the distribution of inflow angles. In future work we want to use the LES results to study the development of the vertical kinetic energy flux, which is crucial for the power production in the fully developed regime of the wind-farm (26) and want to compare the results with various engineering models.

Acknowledgements: This work is funded in part by the research program 'Fellowships for Young Energy Scientists' (YES!) of the Foundation for Fundamental Research on Matter (FOM) supported by the Netherlands Organization for Scientific Research (NWO), and in part by the US National Science Foundation, grants # CBET 1133800 and OISE 1243482. The computations have been performed on our local cluster and the LISA cluster of SARA in the Netherlands.

References

[1] Half-year report 2011. World Wind Energy Association. August 2011.

[2] Commission of the European Communities. *A European strategic energy technology plan - technology map*, 2007.

[3] U.S. Department of Energy. 20% *wind energy by 2030: increasing wind energy's contribution to U.S. electricity supply*, U.S. Department of Energy, 2008.

[4] Wind in Power, 2011 European statistics, The European wind energy association, February 2012.

[5] D. Keith, J. DeCarolis, D. Denkenberger, D. Lenschow, S. Malyshev, S. Pacala, and P. J. Rasch, *The influence of large-scale wind power on global climate*, Proc. Natl. Acad. Sci. U.S.A. **101**, 16115 (2004).

[6] C. Wang and R. G. Prinn, *Potential climatic impacts and reliability of very large-scale wind farms*, Atmos. Chem. Phys. **10**, 2053 (2010).

[7] S. Baidya-Roy, S. W. Pacala, and R. L. Walko, *Can large scale wind farms affect local meteorology?*, J. Geophys. Res. **109**, D19101 (2004).

[8] D. Barrie and D. Kirk-Davidoff, *Weather response to management of large wind turbine array*, Atmos. Chem. Phys. Discuss. **9**, 2917 (2009).

[9] L. Zhou, Y. Tian, S. Roy, C. Thorncroft, L. F. Bosart, and Y. Hu, *Impacts of wind farms on land surface temperature*, Nature Clim. Change **2**, 539 (2012).

[10] B. Sanderse, S. P. van der Pijl, and B. Koren, *Review of computational fluid dynamics for wind turbine wake aerodynamics*, Wind Energy **14**, 799 (2011).

[11] L. Vermeer, J. Sorensen, and A. Crespo, *Wind turbine wake aerodynamics*, Progress in Aerospace Sciences **39**, 467 (2003).

[12] A. Jimenez, A. Crespo, E. Migoya, and J. Garcia, *Large-eddy simulation of spectral coherence in a wind turbine wake*, Environ. Res. **3**, 015004 (2008).

[13] A. Jimenez, A. Crespo, and E. Migoya, *Application of a LES technique to characterize the wake deflection of a wind turbine in yaw*, Wind Energy **13**, 559 (2010).

[14] J.-O. Mo, A. Choudhry, M. Arjomandi, and Y. Lee, *Large eddy simulation of the wind turbine wake characteristics in the numerical wind tunnel model*, Journal of Wind Engineering and Industrial Aerodynamics **112**, 11 (2013).

[15] C. Li, S. Zhu, Y. Xu, and Y. Xiao, *2.5D large eddy simulation of vertical axis wind turbine in consideration of high angle of attack flow*, Renewable Energy **51**, 317 (2013).

[16] L. A. Martinez, S. Leonardi, M. Churchfield, and P. Moriarty, *A comparison of Actuator disk and actuator line wind turbine models and best practices for their use*, 50th AIAA Aerospace Sciences Meeting including the New Horizons Forum and Aerospace Exposition (2012).

[17] J. E. Cater, S. E. Norris, and R. C. Storey, *Comparison of Wind Turbine actuator methods using Large Eddy Simulation*, 18th Australasian Fluid Mechanics Conference Launceston, Australia 3-7 December 2012 (2012).

[18] N. Troldborg, J. Sorensen, and R. Mikkelsen, *Numerical simulations of wake characteristics of a wind turbine in uniform inflow*, Wind Energy **13**, 86 (2010).

[19] N. Troldborg, G. C. Larsen, H. A. Madsen, K. S. Hansen, J. N. Sorensen, and R. Mikkelsen,

Numerical simulations of wake interaction between two wind turbines at various inflow conditions, Wind Energy **14**, 859 (2011).

[20] R. C. Storey, S. E. Norris, K. A. Stol, and J. E. Cater, *Large eddy simulation of dynamically controlled wind turbines in an offshore environment*, Wind Energy **doi: 10.1002/we.1525**, (2012).

[21] S. Ivanell, Ph.D. thesis, Dept. of Mechanics, Gotland Univ., Stockholm, Sweden, 2010.

[22] M. J. Churchfield, S. Lee, P. J. Moriarty, L. A. Martinez, S. Leonardi, G. Vijayakumar, and J. G. Brasseur, *A Large-Eddy Simulation of Wind-Plant Aerodynamics*, 50th AIAA Aerospace Sciences Meeting including the New Horizons Forum and Aerospace Exposition AIAA 2012 (2012).

[23] M. J. Churchfield, S. Lee, J. Michalakes, and P. J. Moriarty, *A numerical study of the effects of atmospheric and wake turbulence on wind turbine dynamics*, Journal of Turbulence **13**, 132 (2012).

[24] S. Lee, M. Churchfield, P. Moriarty, J. Jonkman, and J. Michalakes, *Atmospheric and Wake Turbulence Impacts on Wind Turbine Fatigue Loadings*, 50th AIAA Aerospace Sciences Meeting AIAA 2012 (2012).

[25] J. Meyers and C. Meneveau, *Large eddy simulations of large wind-turbine arrays in the atmospheric boundary layer*, In 48th AIAA Aerospace Sciences Meeting Including the New Horizons Forum and Aerospace Exposition, Orlando, Florida Art. no. AIAA2010 (2010).

[26] M. Calaf, C. Meneveau, and J. Meyers, *Large eddy simulations of fully developed wind-turbine array boundary layers*, Phys. Fluids **22**, 015110 (2010).

[27] M. Calaf, M. B. Parlange, and C. Meneveau, *Large eddy simulation study of scalar transport in fully developed wind-turbine array boundary layers*, Phys. Fluids **23**, 126603 (2011).

[28] R. Cal, J. Lebrón, L. Castillo, H. Kang, and C. Meneveau, *Experimental study of the horizontally averaged flow structure in a model wind-turbine array boundary layer*, J. Renewable Sustainable Energy **2**, 013106 (2010).

[29] X. Yang, S. Kang, and F. Sotiropoulos, *Computational study and modeling of turbine spacing effects in infinite aligned wind farms*, Phys. Fluids **24**, 115107 (2012).

[30] Y.-T. Wu and F. Porté-Agel, *Large-Eddy Simulation of Wind-Turbine Wakes: Evaluation of Turbine Parametrisations*, Boundary-Layer Meteorol **138**, 345366 (2011).

[31] Y. T. W. and. F. Porté-Agel, *Simulation of Turbulent Flow Inside and Above Wind Farms: Model Validation and Layout Effects*, Boundary-Layer Meteorol **146**, 181 (2013).

[32] R. J. A. M. Stevens, J. Graham, and C. Meneveau, *A concurrent precursor inflow method for Large Eddy Simulations and applications to finite length wind farms*, submitted to Renewable Energy (2013).

[33] E. Bou-Zeid, C. Meneveau, and M. B. Parlange, *A scale-dependent Lagrangian dynamic model for large eddy simulation of complex turbulent flows*, Phys. Fluids **17**, 025105 (2005).

[34] R. J. Barthelmie, K. Hansen, S. T. Frandsen, O. Rathmann, J. G. Schepers, W. Schlez, J. Phillips, K. Rados, A. Zervos, E. S. Politis, and P. Chaviaropoulos, *Modelling and Measuring Flow and Wind Turbine Wakes in Large Wind Farms Offshore*, Wind Energy **12**, 431

(2009).

[35] R. Barthelmie, O. Rathmann, S. Frandsen, K. Hansen, E. Politis, J. Prospathopoulos, K. Rados, D. Cabezn, W. Schlez, J. Phillips, A. Neubert, J. Schepers, and S. van der Pijl, *Modelling and measurements of wakes in large wind farms*, Journal of Physics: Conference Series **75**, 012049 (2007).

[36] R. Barthelmie, S. Frandsen, O. Rathmann, K. Hansen, E. Politis, J. Prospathopoulos, J. Schepers, K. Rados, D. Cabezn, W. Schlez, A. Neubert, and M. Heath, *Measurement on a wind turbine wake: 3d effects and bluff body vortex shedding*, Report number Ris-R-1765(EN) (2011).

[37] J. G. Schepers, Ph.D. thesis, Delft University, 2012, doi:10.4233/uuid:92123c07-cc12-4945-973f-103bd744ec87

[38] J. Meyers and C. Meneveau, *Optimal turbine spacing in fully developed wind farm boundary layers*, Wind Energy **15**, 305317 (2011).

[39] T. Burton, D. Sharpe, N. Jenkins, and E. Bossanyi, *Wind Energy Handbook* (John Wiley & Sons, New York, 2001).

[40] R. J. A. M. Stevens, D. F. Gayme, and C. Meneveau, *Large Eddy Simulation studies of power output in large wind farms: effects of wind farm length and turbine placement*, to be submitted to J. Renewable Sustainable Energy (2013).